Journal of Techniques, ISSN: 2708-8383, Vol. 5, No. 3, 2023, Pages 143-157
DOI: https://doi.org/10.51173/jt.v5i3.1451

JOURNAL OF TECHNIQUES

Journal homepage: http://journal.mtu.edu.iq

REVIEW ARTICLE - ENGINEERING

Evaluating The Approaches of the 3D Models Generation of a Soil Surface: A Review Study

Shaimaa Hailem Teamaa[1*], Jasim Ahmed Ali AL-Baghdadi[1], Farid Majid Abd[1]

[1] Engineering Technical College - Baghdad, Middle Technical University, Baghdad, Iraq

[*] Corresponding author E-mail: shaimaahailem12@gmail.com

Article Info.

Article history:

Received
20 April 2023

Accepted
30 July 2023

Publishing
30 August 2023

Abstract

There are various approaches used to create 3D models of soil surfaces, including field surveying, photogrammetry and laser scanning methods. However, most of these methods are high cost, requiring many employees and long processing time. Thus, this study will evaluate these approaches and will show the merits and the significances of each approach used for 3D soil generations. The review study shows that the videogrammetric method is considered the efficient approach for 3D soil surface generation because it is economic, precise, fast, and needs few workers.

Publisher: Middle Technical University

Keywords: Videogrammetric Technology; Close Range Photogrammetry; 3D Models Soil Surface.

1. Introduction

This paper provides an overview of the most widespread techniques for producing accurate 3D digital representations of the soil surface, quantifying the variance in surface properties, and obtaining accurate 3D coordinates for any surface point. There are several methods for creating 3D models, some of which will be discussed in this paper. Examines and discusses the available techniques for building a 3D model using different technologies and platforms. Among the most important traditional techniques used to create 3D models of soil surfaces are terrestrial laser scanning, drone scanning technology, photogrammetry close-range, and videogrammetry technology. This paper presents the methodologies used for each technique, device, equipment, and, most important, the programs used for office processing and presents the results obtained by the researchers. Traditional photogrammetry technology only sometimes meets the market's demand for rapid production. Complexity arises when used on bulky objects, resulting in high cost, time, and tiresome labor. The paper presents the possibilities of using a non-metric mobile phone video camera “videogrammetry” to create a metric 3D model of engineering objects using Agisoft and Cloud Compare software [1].

2. Photogrammetric Technique

To determine the geometric relationship between a three-dimensional (3D) object and a two-dimensional (2D) photographic image, a measurement technique known as near-range photogrammetry is used; The method can also be referred to as the methodology when photographs are used to record the temporal history of an object's spatial coordinates. The photogrammetry technique can be classified as aerial, or ground based on the images excised from the video and analyzed [2]. As the name suggests, it uses photogrammetry technology. Aerial photogrammetry: Pictures taken by aircraft, satellites, or hot air balloons. In contrast, the ground-based photogrammetry method, known as the close-up photogrammetry method, uses images from ground-based cameras. A few civil engineering applications have benefited from close-up photogrammetry methods and soil surface surveys.

3. Videogrammetry Technique

"videogrammetry" refers to obtaining accurate 3D data from video photos. Videogrammetry can also refer to the term "photogrammetry." when it comes extract static image of the scene from recorded video it is a method frequently utilized in various areas, including comprehending the position and orientation of the camera and the location and distance of objects in the scene. The process requires analyzing the video clip or the photographs. Following the collection and processing of the data, a three-dimensional model of the location or object under investigation is

Nomenclature & Symbols			
CRP	Close-Range Photogrammetry	GCPs	Ground Control Points
2D	Two Dimensions	UAV	Unmanned Aerial Vehicle
3D	Three Dimensions	RMSE	Root Mean Square Error
SfM	Structure From-Motion	OTS	Optical Triangulating Laser Scanner
RMSH	Root Mean Squared Height	IOP	Internal Orientation Parameters
f	Focal Length	SD	Standard Deviation
TLS	Laser Scanning Technology	CPS	Controlled Photogrammetry System

generated. Compared to more conventional surveying techniques, this technology is making rapid strides toward improvement and is gaining popularity due to its adaptability, precision, and lower overall cost.

3.1. Videogrammetric algorithms

The main goal of any photographic project is to figure out the 3D and the coordinates (x, y, z) of the points on any object, as well as to get the camera parameters (IOP) and the external orientation parameters (EOP). Video metering, in general, can be done in many different ways. Find out an object's 3D locations for two or more points. In photogrammetry, you can get more than one sync frame by editing synchronized video clips. Changes to a package can be used to make What three-dimensional space has to do with two-dimensional projections. The experts found that the collinear equation model worked well. The best math formula for this kind of app to measure videos are, these equations are called "linear equations," and the condition of a linear relationship is that the lens capture Centre, the picture point, and the object point must all be on the same line [3] as the shown Fig. 1.

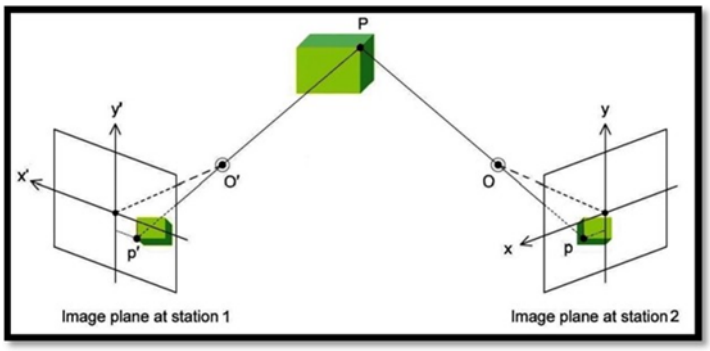

Fig. 1. Principles of centripetal projection

3.2. Base to height ratio (B/H)

To achieve a realistic and ideal photographic measurement Digital picture resolution in any CRP project, Aspect ratio (B/H) is a required rule. The horizontal distance between the camera stations is supplied, as is the height. It should represent the distance from the camera station to the surface or object. Photographer When planning any CRP Project, it is critical to consider the parameters that influence the camera to object distance (H), which is the most essential variable. These variables are classified into two categories. The first kind includes elements that prohibit the camera from reaching the target, such as the camera's depth of field and the number of picture points on the object. The second type of factor comprises factors that prevent the camera from moving away from the target, such as picture resolution, image scale, and field of view. [4] define the camera and workspace. A short baseline can result in a tiny base/height (B/H) ratio, which is geometrically undesirable due to a bad intersection angle resulting in a big depth inaccuracy. Furthermore, as illustrated in Fig. 2, Wide base imaging provides improved positional resolution.

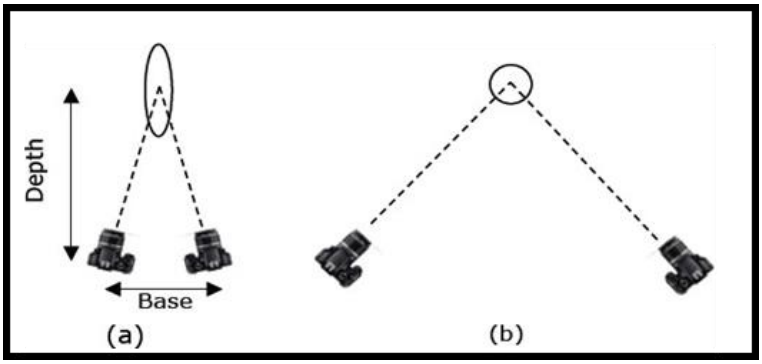

Fig. 2. Imaging geometry (a) Low B/H ratio and significant error. (b) a high B/H ratio with low error [4]

4. Surface Soil

Scientists have used various methods to get detailed information about the height of the soil to find surface boundary processes [5] say that these methods require that the measuring device touch the soil, which could disturb the soil. Laser scanning terrestrial and stereographic are

good technology to measure the height of the soil's surface without touching it. Even though laser technology is the most accurate, stereo imaging costs less at first because digital imaging technology has improved. One of the best things about stereo photogrammetry is that it has become easier to use over time. This is thanks to the development of high-quality digital cameras for consumers and powerful algorithms for image processing and camera calibration. Even though the steps for image processing and camera calibration have been made much easier, this technologic still depends on getting control points that are accurately measured. Different ways have been suggested to make the field survey steps less time-consuming. This paper aims to look at the most important techniques used to figure out how accurate and sensitive stereogrammetric is at finding changes in the height of the soil surface by comparing the DEM with the data extracted from the laser scanner technique [6].

5. Modeling Using Laser Scanning Technology (Create 3D Models of Soil Surface)

The development of micro-imaging parameters of soils that can be correlated with reflectance data or structure derived DEMs from movement in both the laboratory and the field and their relationship to erosion can be accomplished through studies using high-resolution Terrestrial laser scanning (TLS). This is made feasible by the quick development of equipment that are now available and reasonably priced, such smartphones, high-resolution cameras, unmanned aerial vehicles, and related digital photography by the creation of precise micro-imaging parameters and the gathering of data in the field, there is a sizable chance to progress soil models [7]. There are many studies used laser scanning technology for 3D soil surface modeling such as:

Milutin Milenkovic (2015), In this study, the researcher discussed the use of laser scanning technology to assess the soil surface roughness on a plot of land measuring (2.6 m* 3 m), as well as the preservation of the DEM construction approach on random surface properties at high frequencies. The researcher also demonstrated how the Height and Roughness Index (RMSh) was scanned using an OTS trigonometric scanner model ser on a sub-plot measuring (0.18 m * 1 m) a wide lens with an 8 mm focal distance was used to scan the area while the OTS scanner was positioned at 0.7 m relative height. This produced ground pixels that were (0.7 mm) in size and a rectangular body coverage of (0.4 mm * 0.3 mm). According to the study, terrestrial laser scanning can measure roughness on scales larger than 5 cm in 70% of scans. Roughness measurement is difficult on small sizes, as shown in Fig. 3 To reduce the footprint of the laser beam [8].

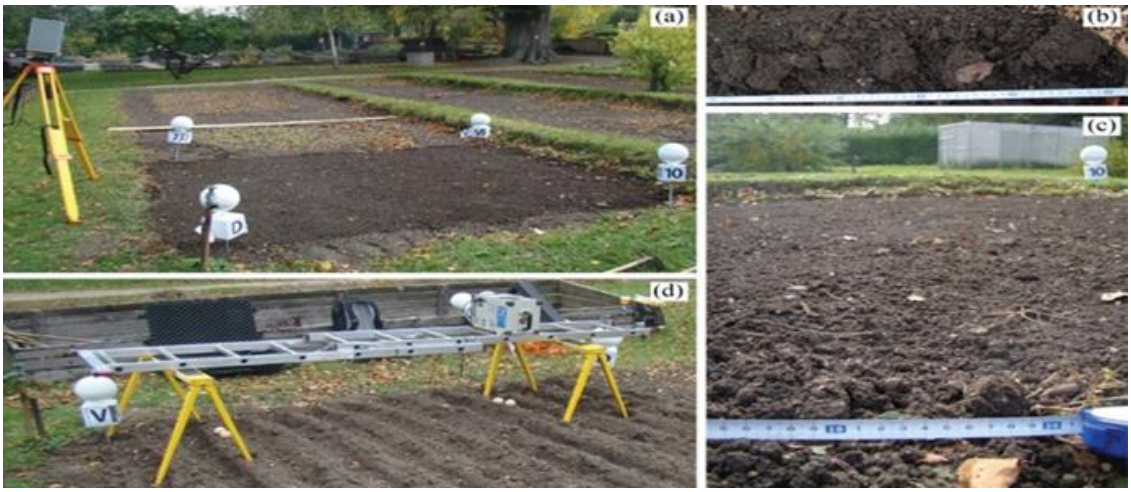

Fig. 3. (a) TLS instrument measurement setting across the investigated plot, (b, c) soil aggregates and other roughness components inside the plot, (d) optical triangulating scanner (OTS) instrument measurement configuration [8]

Nouwakpo, S. K., and others (2016), in this study, the researchers talked about how SfM and TLS techniques for microscopic soil reconstruction worked on erosion plots (6 m x2 m) with 0% to 77% vegetation cover. Images used for SfM reconstructions were taken with a Canon EOS Digital Rebel XT camera with a fixed nominal focal length of (20) mm. The researchers used 15 grid control points in each plot and focused the camera lens by hand after adjusting for the average distance of the camera and the 2m surface of the soil. SfM reconstructions could be done with the help of PhotoScan software (Agisoft). Because this study used a single-point-of-view laser scanning method, the researchers found that plants blocked the soil surface more with TLS than with SfM. TLS can be used to build models of different heights, but these devices weren't widely used because they were too expensive and too big. On the bare soil surface, as shown in Fig. 4, the researchers used GCP targets, which are (5 cm) plastic squares with a checkerboard pattern and (15) cm anchor pins attached to them. A Nikon NPR 352 total station is used to find GCP coordinates.

In this study, the accuracy of NPR 352 was (0.4) mm vertically and 3 mm horizontally, on average. The estimated height values from SfM were within 5 mm of those from TLS, but SfM did show long-distance distortions. The agreement between SfM and TLS got a little worse as the percentage of land covered with plants increased, but it worsened after 53% from of vegetation. The researchers used Cloud Compare V2.5 to compare the two and as shown in Fig. 5, used recorded point clouds to compare SfM and TLS results from the tests. Each TLS scan took about (15) minutes and looked at a (6m*2m) (plot) area. It took at least an hour to look over each plot.

On the other hand, each plot had to be scanned to re-build the SfM. It takes just 15 minutes. TLS makes a lot of points that can be looked at right away. On the other hand, SfM data comprises images that overlap and must be turned into a 3D point cloud. The GCP image coordinates had to be measured for a reliable conversion to metric coordinates. Compared to TLS, SfM might be a cheaper field research method. This is because the millimeter scale measures changes in soil microscopy. It could happen when the TLS tool moves between scanning sites, as shown in Fig. 6 [9].

Liu, L.et al (2022), this study discusses how to employ laser scanning to get a 3D digital model of the surface during an internal clearance test, as well as the impact of roughness. As a result, there are four sets of trench depths and two distinct kinds of surface conditions. After trenching, laser radar is used to determine the 3D height of the soil's surface. The researcher constructed a soil box 4 meters long and 0.8 meters broad at the Midwest Comprehensive Building of Anhui Agricultural University, as shown in Fig. 7. Before and after plowing, the researcher excavated holes in the (200 mm, 400 mm, 600 mm) long, and (10) cm deep soil. He sent data as a "point cloud" to a portable computer, subsequently processing it. MATLAB software to generate a digital model of the soil surface. The findings revealed that when the drilling depth varied, so did the RMSH values, as shown in Fig. 8 [10].

Fig. 4. Ground laser scanner [9]

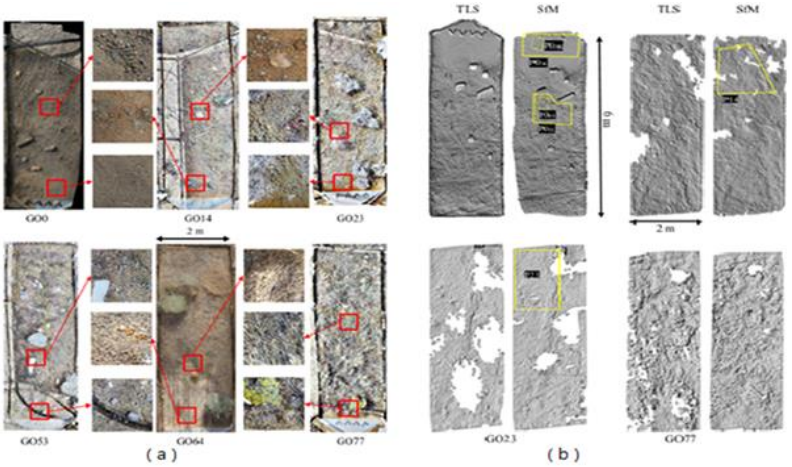

Fig. 5. (a) An overview of plots go0, go14, go23, go53, go64, and go77, as well as close-up views of each. About 0.6m by 0.6m long, each close-up view window, (b) Examples of reconstructed bare ground surfaces using terrestrial laser scanning (TLS) and structure-based modeling. The white holes show where there are few or no points in the from-motion data (sfm). The solid and dashed yellow polygons show the shapes of the detail cloud comparison patches. The space between each grid is 1 millimeter [9]

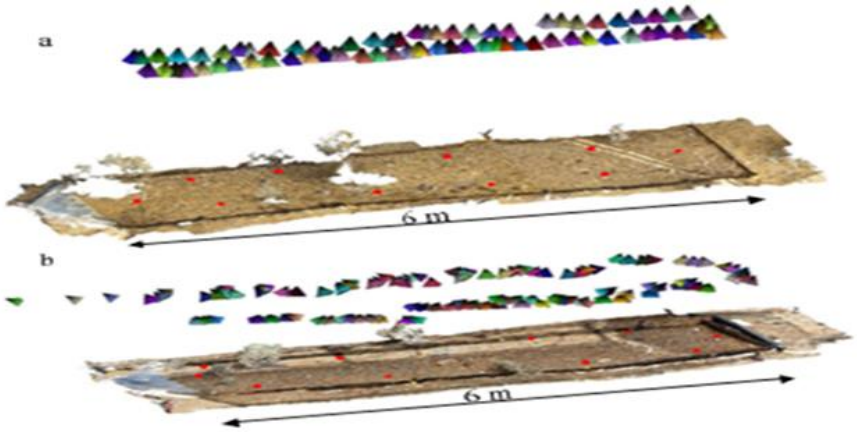

Fig. 6. Shows a side view of three-dimensional reconstructions using image networks for; (a) camera-on-pole and (b) ground-based camera setups. Red dots show where ground control points are [9]

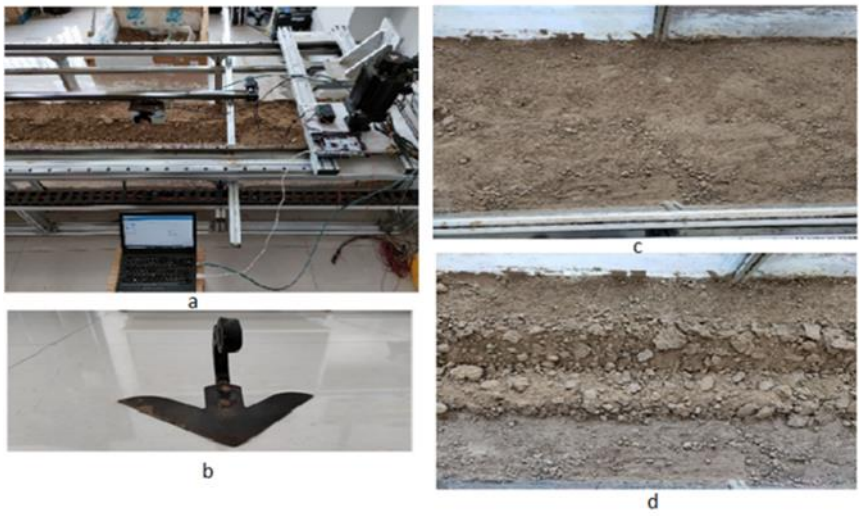

Fig. 7. a) Measuring device, b) Ditching shovel, c) Initial landform, d) Landform after ditching [10]

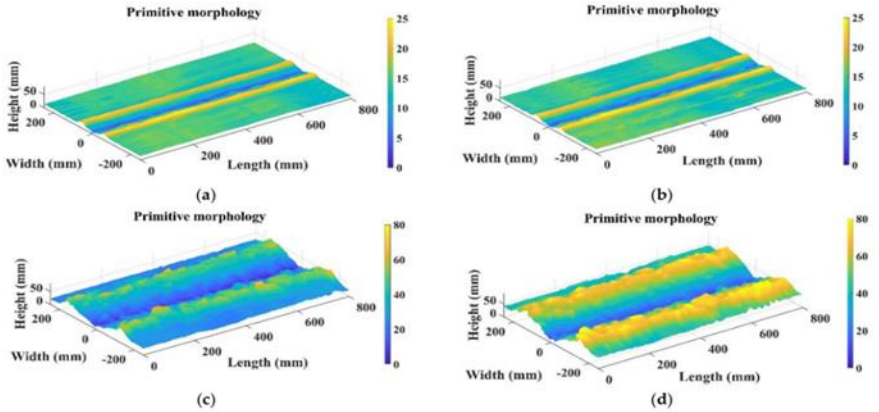

Fig. 8. Digital model of soil surface; (a) Ditching depth of 5 cm, (b) Ditching depth of 8 cm, (c) Ditching depth of 10 cm, (d) Ditching depth of 12 cm [10]

5.1. 3D models using UAV photogrammetry of soil surface

This technology is now considered the simplest way for 3D soil surface modeling among the other approaches. Unmanned aerial vehicles (UAVs) can be used for geo-risk assessment thanks to photogrammetry, drones, and the architecture of SfM (digital photogrammetry architecture) [11, 12]. Drones can have a variety of sensors, including photogrammetry, which is necessary for creating the 3D model. Using drones equipped with high-resolution cameras can be a manageable financial investment. The TLS module is significantly accuracy, but they produce point cloud data that is almost identical to one another. Many researchers introduced a method that allows them to create high-resolution 3D models even when using UAVs with a low resolution. Setting up unmanned aerial vehicles (UAVs) and collecting images is much simpler when commercial mobile apps are used for autonomous flight planning. Using drones for blocking because they can take high-quality pictures of rocks from various angles, such as the plane view, tilt front view, side view, and close-up views from a safe distance. Examples of these types of views include the plane, tilt front, and side views. This technology is superior to laser scanning regarding safety and locating large bumps because it can do both things. Most quadcopters available for purchase weigh less than 2 kilograms and can be carried in a backpack [13]. The primary photogrammetry software currently on the market for processing can take anywhere from two hours to several days, depending on the number of images, their resolution, and the computational power of the PC. Now, Software packages like Agisoft, Pix4D, Autodesk, and Bentley offer the benefit of relatively faster cloud processing, which saves money on hardware costs. Inclement weather, such as precipitation or strong winds, makes aerial photography more difficult, and snowfall can significantly degrade the quality of the captured images.

Additionally, the angle at which the sun is shining influences the number of shadows captured in the images, which can cause noise in the precise 3D models. The hardware costs are reduced, and it is relatively faster. Therefore, several studies focused on using UAV for 3D soil surface modeling, such as:

kaźmierowski, c, et al (2015), the researcher explained how to use photogrammetry to generate a digital elevation model, as shown in Fig. 9. The Figure depicts the processing of (127) aerial pictures obtained using a drone hexacopter from a height of roughly 10 meters above ground level of the designated area in the Polish county. The authors captured the photographs with a Sony Alfa 6000 24 Megapixel camera array. They marked four locations on the image using Topcon Geodetic GPS, which has an accuracy of roughly 1 mm (horizontal and vertical) in National Coordinate System 2000 Region 6. (No. 2177 of the EPSG) With Agisoft Photoscan Professional 1.1.6, do metric image processing before calculating using GrassGIS. Three traditional metrics derived directly from the DEM are shown in Fig. 10. The DEM standard deviation, the residual standard deviation, and the standard deviation of good faith Processing of Output with Photoscan, creating a digital elevation model.

To construct geo-patterns for each pixel and average all models on a (1 x 1) m spatial grid, use the Grass GIS r.geomorphon extension. The average pixel size of the digital pictures utilized for photogrammetry was determined to be around 0.25 cm. The estimated point cloud has around (12) million points, at a density of 19,500 points per square meter. Examine the data using a GIS program that employs filtering. The least curvature approach was used to calculate the point cloud noise of a digital elevation model, as illustrated in Fig. 11; the pixels have a spatial resolution of one centimeter [14].

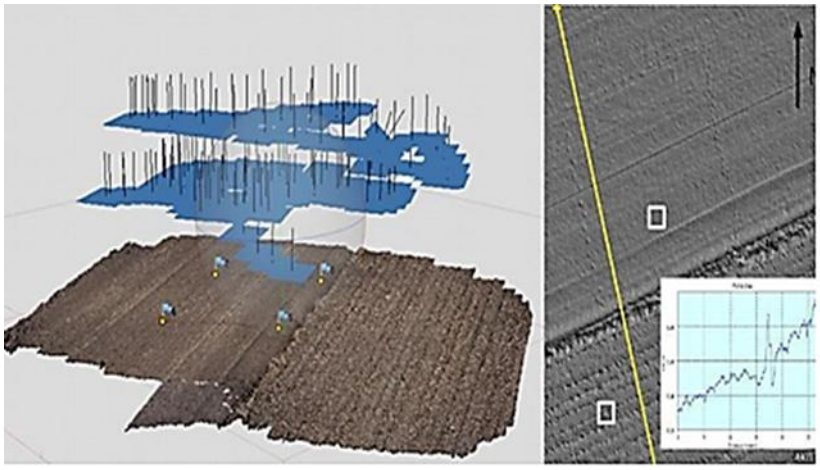

Fig. 9. Layout of aerial images (blue rectangles) with produced point cloud (left) and coloured terrain with transaction indicating height above sea level (right) Rectangular highlights examples of area for roughness indices computation [14]

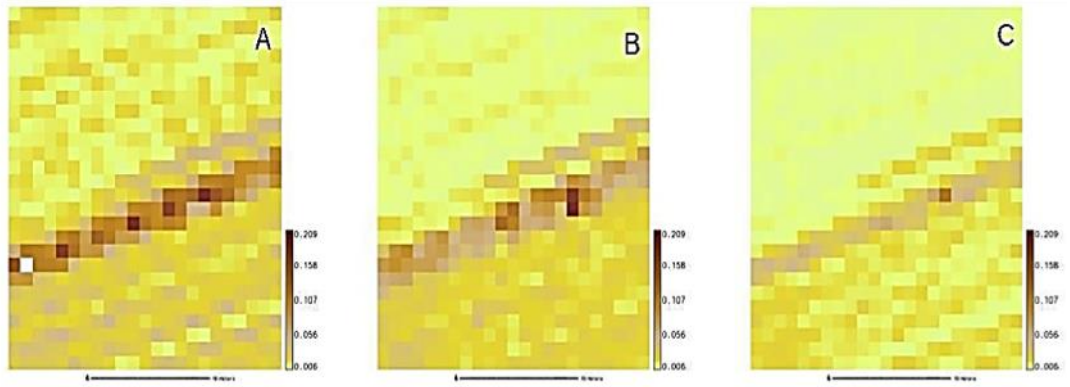

Fig. 10. Three different ways to measure roughness; (A) the standard deviation of DEM, (B) the standard deviation of prominence, and (C) the standard deviation of residuals [14]

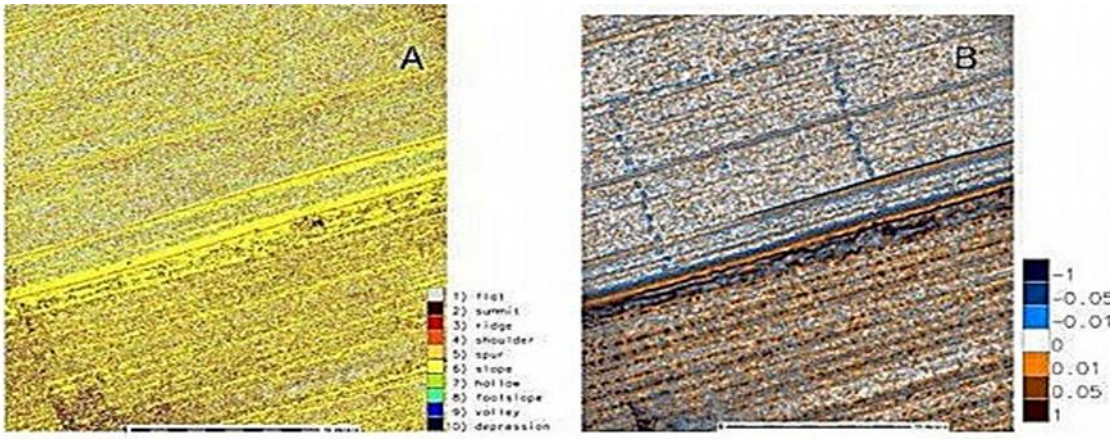

Fig. 11. Models created using the geomorphons method: (A) landform classes and (B) exposure [14]

5.2. Digital photogrammetric modeling using close-range photogrammetry (CRP method)

Utilizing digital technology for photogrammetry, the traditional method of creating topographic maps using photogrammetry, in which overlapping photographs are projected in stereo pairs to create a three-dimensional image, is the foundation for the modern digital photogrammetry technique. Automation of photogrammetry is accomplished through the use of digital photography and computer processing. This digital procedure is gaining popularity due to its lower cost and approach to testing that does not involve contact [15]. This method requires photographs of the soil surface from various perspectives, with a sixty to eighty percent overlap between the side and frontal views. In spite of

the fact that photogrammetry can reconstruct a three-dimensional model of a visual object from as few as two photographs, an excessive number of pictures is necessary to cut down on modeling errors and eliminate blind spots. It is essential to obtain clean and precise soil photographs to create accurate 3D photographs, which can then be used as the basis for creating 3D models [16]. The photogrammetric method has been used to record and measure surface area and volume changes. It has been demonstrated that it can produce highly accurate results when digital cameras are utilized. Several previous studies used the photogrammetric method for 3D soil surface modeling are:

Dirk H. Rieke-Zapp (2005), this study shows how to create digital elevation models (DEM) of soil surfaces over large areas and use digital photogrammetry to measure digital soil erosion. A digital camera made for consumers was used in this study to take pictures. The researcher uses BLUH and DPCOR software to calibrate the camera (2000). The researcher used about 20 images to calibrate the software and build it to work on images whose orientation is unknown. The researcher set up a rain experiment in a (4 x 4 x 0.8) m^3 stream to find out how the shape of a slope affects soil erosion. The object is made from two adjacent holograms to test how well their coordinates match. With a 60% overlap in front, there was a 20% overlap on the side.

The average difference between the Z values is close to zero. The results were found by comparing the coordinates. which shows that the dataset has only a tiny amount of bias. Estimates of the overall accuracy of (1–26) mm in the vertical position the researcher sees meet the project's needs. Still, they fall short of the theoretical accuracy that could be calculated by error propagation. They also don't match the exact estimates of comparative studies [17,18]. The researcher concluded that these two studies were based on different research goals at different levels. DEM was created with a 3 mm f level of accuracy. In the vertical position, a resolution of about 1 mm is more than enough to meet the goals of the wear measurements done in this experiment. The CCD sensor has a (3060 x 2036) image element (pixel) matrix, and the best image quality was achieved with the aperture set to f/9-5. The results showed that the coordinates of the target image were more accurate by more than (0.02) pixels. RMSE = (0.235) was the difference between the length of the scale bar that was seen and the length that was gotten from the model. Each pixel was (0.009) mm long. As shown in Fig. 12, the RMSE for differences between control sites along the X-axis is (0.031) mm, and along the Y-axis, it is 0.042 mm [19].

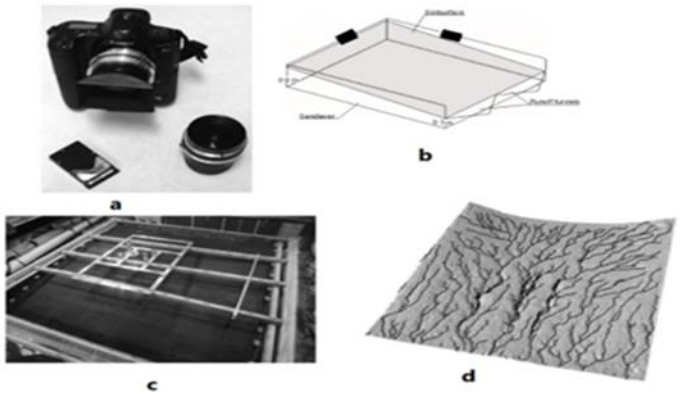

Fig. 12. a) Kodak DCS1m with Leica 19 mm lens and Schneider 28 mm lens in foreground. b) experimental flume (4 x 4 x 0.8 m^3) d) hill-shading model of one soil surface DEM exaggerated three times in Z From the DEM, the surface rill network was superimposed [19]

Kinarsari, A.E. et al. (2017), the researchers discussed the method of close-range photogrammetry and Agisoft PhotoScan software to create 3D impressions of tractor tires on the soil. Gabion baskets were (3 * 3 * 1)meters. Michigan Tech's Department of Civil and Environmental Engineering has done this study. A Sony Mirrorless Digital Camera with a 35 mm focal length and image resolution of (6000 x 4000)pixels was used to create a 3D model of the soil surface using photogrammetry with 60-80% end and side overlap 3D images of the soil surface before and after a tired pass were used to create a DEM. For model evaluation, three Nikon DSLR D3300 digital cameras on a frame-mounted trolley were employed to take continuous frame print images. The researcher fixed 39 markers and ground control positions to simulate a three-meter tire track. The two 3D models were imported in TIF format into MATLAB for soil deformation analysis. The two types of tire grooves were examined. It was found that the photogrammetric approach can measure the size of the fracture, the surface area, and the depth. The study results are the accuracy of the photogrammetry on a large range. Two sand cone tests estimated volume in the (4-7)% range of the photogrammetry. The photogrammetry test included inserting a small tin into the sandy soil and measuring its volume, surface area, and depth. Calculations of modest soil volumes match body size. Errors of (6.7)% and(0.2)% in item size and dimensions. Lighting was necessary because dark organic soil reflects less light than sandy soil. Ghosting degrades frame fingerprint images, as shown in Fig. 13 the work methodology used [20].

Grundy, L., et al (2020), this research shows using a 3D camera for 3D soil surface creation. Intel RealSense Depth Camera was the 3D camera (model D415). The camera is compact and lightweight (72g) (99mm x 23mm x 20mm). The camera was mounted on an aluminum frame, and a tripod enabled it to be lifted above the surface from 1,500 mm to 750 mm. Then, take photos from six heights ranging from 1500mm to 750mm. In this experiment, the 3D camera is a depth-regulated light camera comprising multiple components aiming at the same field of view. The camera collects data at both visible and infrared (IR) wavelengths. The camera's infrared emitter has a well-organized pattern. The researcher used a visible light receiver and two infrared sensors attached to a stereo to capture infrared and visible light data from the camera's overall field of view. The distance between the camera and the surface represents the depth values. The camera can take data at a resolution of 1280 x 720 pixels from a surface at a range of 0.45 m to around 10m, with accuracy varied based on calibration, camera-to-object distance, and calibration, and camera-to-surface distance. Target item type in the picture, and lighting conditions.

The camera is pre-calibrated, but the use of stereo image sensors distinguishes this camera from its competitors. By using a single sensor, you may get greater depth accuracy. The photos were captured by connecting the 3D camera to a PC through USB 3.1 and an Intel RealSense viewer. Although the camera's resolution was great, it declined as soil distance increased (0.3% at 750 mm and 0.5% at 1500 mm), yet it

remained quite precise (0.5 mm for height and 0.05 mm for random roughness). As shown in Fig. 14, The results show that the surface area estimate error increased with distance (0.56% at 750 mm and 2.3% at 1500 mm). According to the study, the Intel SDK may be used to access, configure, and adjust camera functionality. Using Image Capture, Intel's Python SDK wrapper constructed a script to record 3D point clouds of the soil surface at predefined intervals. As shown in Fig. 15, the 3D camera has a frame rate of 30 frames per second [21].

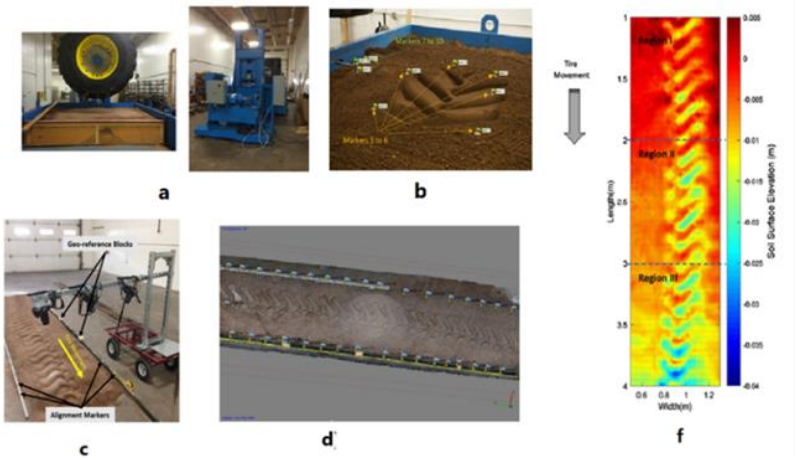

Fig. 13. a) Servo hydraulic static tire loading, b) Imported soil surface and ground control point images into Agisfot PhotoScan Professional, c) Photographing the soil after the tire passes, d) Tire-rolled soil model, f) The rolling tire test's soil imprint [20]

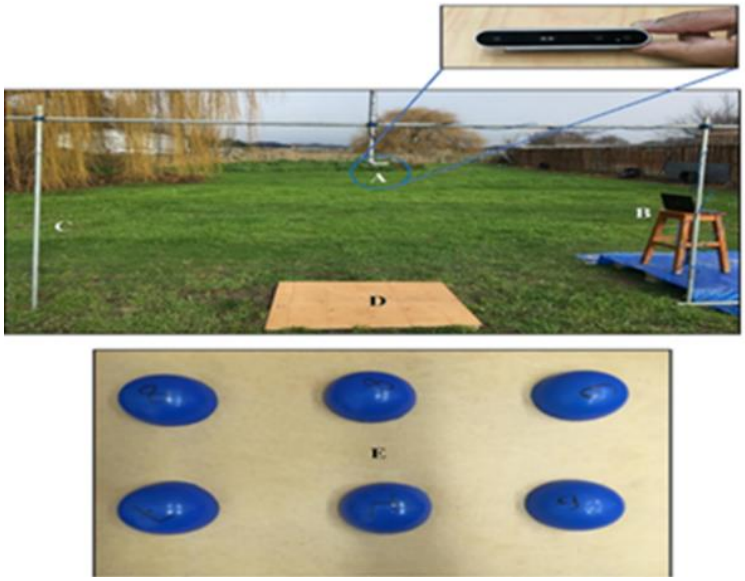

Fig. 14. a) Intel RealSense depth camera, (b) laptop, (c) support legs, (d) plywood imitated smooth soil surface, and (e) plastic hemispheres simulated rough soil surface [21]

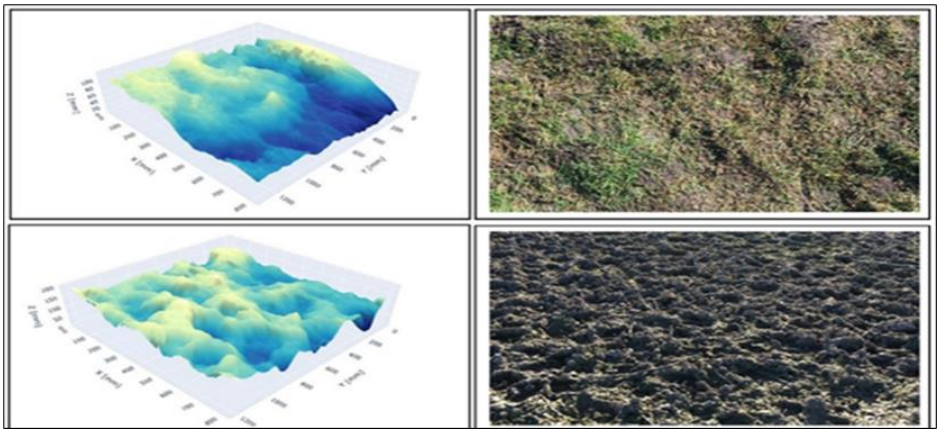

Fig. 15. A 1200 mm * 800 mm region was collected using a 3D camera 1000 mm above the surfaces to create a digital elevation model (DEM; 1 mm * 1 mm) for the complete (upper) and damaged (lower) soil surfaces, processes are described in the Supplementary Material, on the left and right, DEMs and photographs of each soil type are displayed [21]

Suchan, J., & Azam, S. (2021), researchers created a Controlled Photogrammetry System (CPS) utilizing an enhanced SfM technique to capture quantitative and qualitative soil parameters using a model with standard dimensions. The sealed housing reduces ventilation and evaporative losses via the acrylic glass. Make use of the researcher. DSLR D3000's accuracy of (10.2)MP captures high-resolution pictures needed for SfM analysis. Shutter speed = 1/10; F-number = 22. During the picture capture camera, the sample cannot be shifted. Within the housing are the rotating sample stand, thermometer, and hygrometer. Three LED lights are positioned on the ceiling. They create consistent illumination and minimize shadows around the sample. As shown in Fig. 16, this setup produces five horizontal orientation angles (5°, 20°, 35°, 50°, and 65°); 30 minutes to collect about 350 photographs. The target score's root means square error (RMSE) assesses accuracy by retransforming the model's coordinate system in the X, Y, and Z axes. The RMSE value was 0.32-0.58 mm. The 1-pixel threshold error ranged from 0.290 to 0.629 pixels. The camera is connected to a laptop running digiCamControl2, which can capture a shot every 4 seconds. Image quality may be improved by adjusting the aperture, ISO, and shutter speed. The aperture was set at 25 (Focal ratio). The researchers employed image processing, model development using Google SketchUp and Agisoft Metashape Professional, model comparison with Cloud Compare V.2, and line detection with Autodesk Civil 3D. Wet and dry images of the model were used to create two three-dimensional representations of the soil surface. A qualitative study of surface characteristics revealed a 1% difference in volume and area between wet and dry sand samples. Wet sand was stippled, but wet clay was smooth, as shown in Fig. 17 [22].

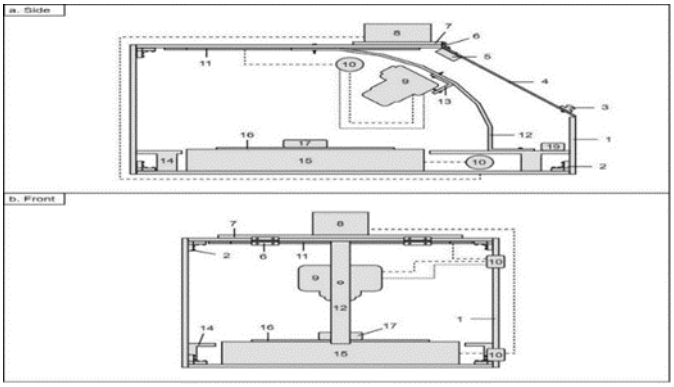

Fig. 16. CPS diagram; (a) left-side viewpoint and (b) front perspective [22]

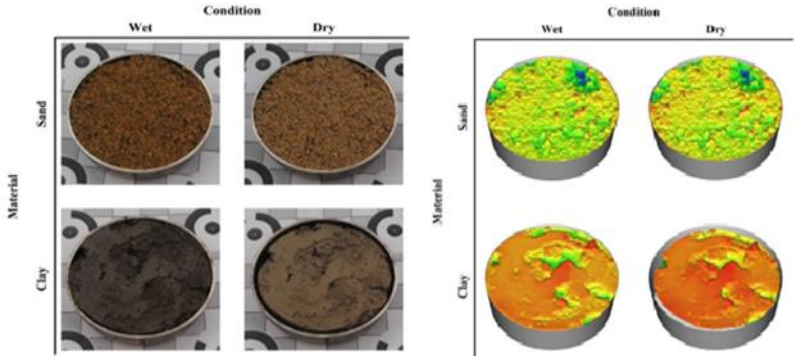

Fig. 17. These are images of sand and clay samples while they are wet and dry, these states are also evaluated qualitatively [22]

Azizi, A. et al 2021, this study explains a computational method for using stereoscopic vision to assess soil roughness in agricultural places using in-field picture data. Soil surface roughness was evaluated using a depth map by estimating the height of plowing blocks. This map was created by isolating and aligning main points as picture super pixels. Coefficients of determination and regression equations display actual and predicted numbers. In 2018, researchers chose and developed the Babulan field 1352 meters above sea level, about 10 kilometers from Ardabil city. The soil was sandy and silty, with an 8% slope. The researchers used stereo-paired photographs to collect information in natural settings. To do so, the W3-Fujifilm stereo camera has a base separation of 7.5cm, a focal length of 12mm, and a resolution of 10MP CCDs for each lens. This camera has a 60-centimeter lens-to-ground clearance. Fig. 18 shows a camera platform design; each of the 156 stereo pairs comprised a 3684 *2736-pixel image. The technique included calibration, rectification, corresponding, and triangulation, allowing crucial imaging equipment to acquire image data quickly. To analyze images more quickly, they were compressed four times. MATLAB R2018a's stereo camera calibrator toolbox uses a checkerboard pattern and camera parameters to calibrate stereo-pair images. The horizontal alignment of the left and right images was achieved after calibration. A three-dimensional point cloud of soil surface was generated, separated by the x, y, and z axes. A computational procedure Image contrast and depth maps were calculated using a microscope technique. The outcome was a collection of seemingly random surface points of soil. Root Mean Square Error (RMSE) X (Pixel)= 1.07, RMSE Y= 1.65, and RMSE XY= as the Fig. 19 [23].

HerodowiczMleczak, et al, (2022), this study shows the way of doing a quantitative analysis of the roughness of different soil surfaces. The researchers discovered an intrinsic association that revealed various information regarding the roughness of the soil surface. They photographed a soil surface devoid of plants using a commercial Sony A7 camera with a 35.8 × 23.9 mm CMOS matrix and a resolution of 24.2 megapixels. They saved the images as high-resolution JPEGs with lens lengths ranging from 18 to 55 mm. A calibration framework is being developed. During the inaugural season, the calibration frame was 1.30 x 1.30 m. The 2*2 frame was made stiffer in the second season to create a surface model with local coordinates. As the chart illustrates, 15 separate photographs were taken of each model, as shown in Fig. 20 that it was. Different the first picture of the plot was taken from a height of about 1.60 meters. The second picture was taken from a height of about 2.30

meters. The range of the digital image was from 0.5 to 2.5 mm (vertical, indirect). Agisoft Photoscan Professional, version 1.2.6, was used to process the data by the researchers. The camera calibration process is applied to eliminate radial distortions. This method is accurate because automated calibration (lining up images) can sometimes give wrong results. The variable focal length by more than 10% between image sets or non-fixed focal length to calculate roughness parameters, make a 3D model, and export in TIFF format with 32-bit floating-point encoding. As the picture shows, each DEM was changed to the GeoTIFF format with a 1 mm spatial resolution., as shown in Fig. 21 [24].

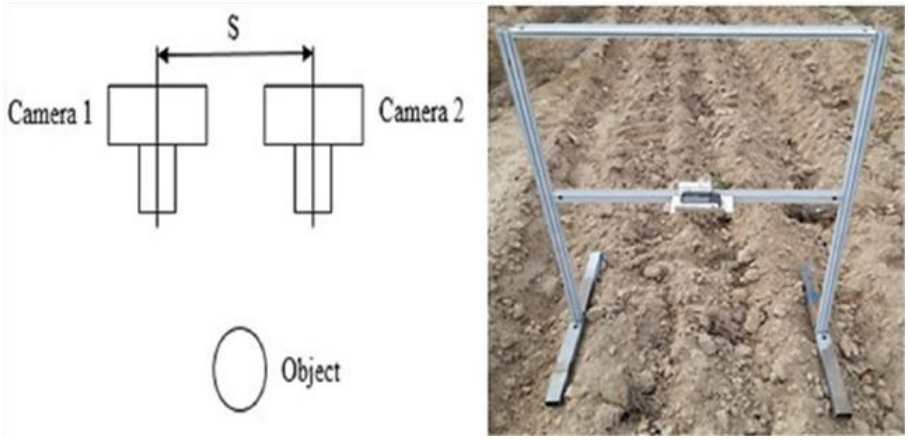

Fig. 18. A diagram of how stereo imaging is set up [23]

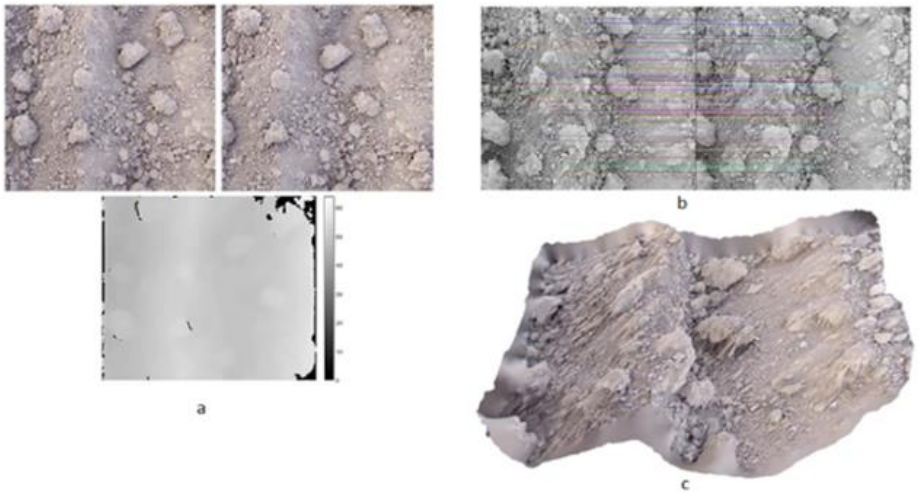

Fig. 19. a) Example of a stereo-pair image with a depth image that goes with it, b) An example of keypoints that have been matched using the brute force algorithm, c) Sample of the 3D model made from the stereo image of the soil surface [23]

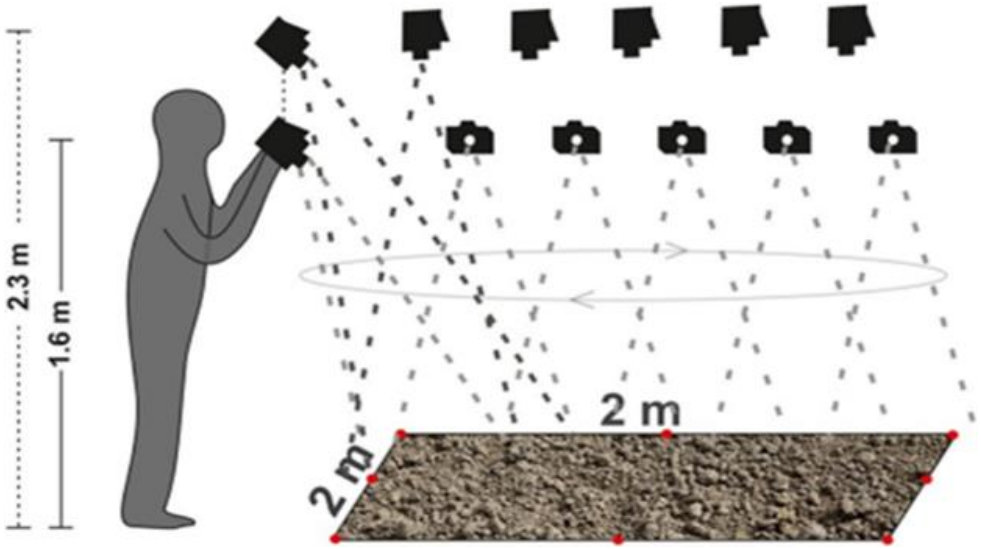

Fig. 20. Acquiring photos for a single plot.[24]

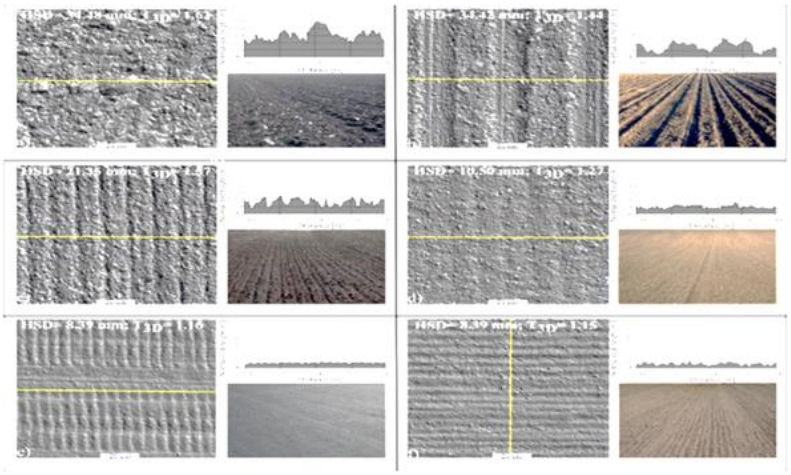

Fig. 21. DEM in Geotiff format with a 1m spatial resolution [24]

5.3. Modeling using videogrammetry (create 3D models of soil surface)

With the advent of high-resolution video sensors that can capture several million pixels in a single frame, videogrammetry has gained significant attention. When video frames are shown sequentially, the frames stack upon one another. This allows for the reconstruction of the scene's 3D surface. If the quality of the initial reconstruction is low, subsequent reconstructions may improve upon it. Full automation of videogrammetric data collecting in outer space is still a work in progress [25]. Videogrammetry is quite similar to photogrammetry. The videogrammetric approach normally consists of four stages: camera calibration, video sequence capture, 2D position measurement of an existing target point or tracking of a new target point in each frame, and 3D reconstruction [26]. Two or more bundled-up cameras are the first step. The depth map and texture measurements of the image are taken from each camera's video frame to determine the 2D coordinates of the target point. The following section will involve the summary of some previous studies that use videogrammetric techniques for 3D soil surface modelling.

(Vinci, A. et al. (2017), in this study, the researcher assessed the usefulness of a smartphone camera for structure-from-motion (SfM) reconstruction to monitor fluctuations in soil surface characteristics and soil loss caused by a low-intensity erosion event. Using ground-based laser scanning (TLS) to validate the SfM model, the researcher chose the Umbria area (20)kilometers south of Perugia (central Italy). The experiment was conducted on a (2m × 11m) plot of land influenced by moderate rainfall. The study utilized an Apple iPhone 6 Plus (4.15mm focal length, 8 MP with 1.5 pixels, f2.2 aperture). The first survey was undertaken before the rain erosion event, whereas the second was conducted after. Two movies were shot in 1080p60 resolution by 1,920 by 1,080p at 60fps while walking around the plot's perimeter from around (2)meters. Using Matlab-developed software to eliminate focal length shifts during video capture. It automatically pulls 2,800 frames (with the exact resolution as the original video, (1,920 * 1,080)pixels - Full HD from video recordings. The placement of thirteen ground control points (GCPs) along fixed plot boundaries and nearby plots is depicted in Fig. 22. The 3D (X, Y, and Z) coordinates of CCPs were gathered using standard ground scanning with a Leica TS06 total station. Initially, a calibration method was established to define the camera settings for Agi soft Lens calibration. Agi Soft Lens use. Flat Grids on an LCD screen measuring 30 inches in size, the calibration grid was presented. Using Agisoft PhotoScan image processing and 3D spatial data production (commercial complete package SfM-MVS), he determined the correctness of SfM point clouds by comparing them to TLS point clouds (used as a reference) Digital Elevation Models (DEMs) (0.01 m * 0.01 m) SfM calculated the measured soil loss precisely, whereas TLS was (26)% off [27].

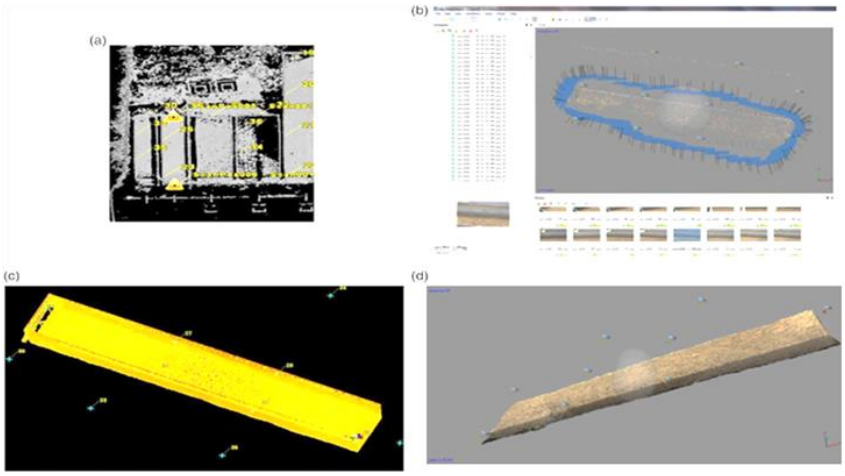

Fig. 22. (a) The triangles represent the locations of the TLS scans and 13 ground control points (GCPs), (b) the alignment frame scheme, (c) the TLS survey model of the 2 11 m plot, and (d) the SfM survey dense point cloud model [27]

5.4. Summary

Table 1 outlines the literature review and approach utilized by the previous researchers to develop three-dimensional models of the soil surface, which were briefly discussed in this work, as well as the outcomes of each technique indicated above.

Table 1. Summary of related studies about 3D models

References	Aim	Methodology	Main Results	Accuracy Assessment Procedure
Milutin Milenkovic (2015) [8]	using terrestrial laser scanning to measure the roughness of the soil surface	• Roughness Preparation Measurement Setup and Acquired Data • Data Processing • Pre-Processing • Data Transformation and Detrending • Roughness Analysis • DEM Generation • Roughness Description • Soil Spatial Correlation and Measurement Noise	The findings that a drop in DEM resolution from 4 mm to 20 mm might result in relative errors in the s and l indices that are more than 5%. DEMs with 12 mm or above spatial resolutions may show the spatial correlation's exponential character. DEMs with 40 mm or below resolutions make the exponentially correlated surface seem Gaussian.	optical triangulating scanner surveyed a 0.18 m by 1 m subplot to measure roughness. TLS and OTS roughness spectra agree at 5 cm spatial wavelength, according to the study. Consequently, TLS can easily evaluate roughness on bigger sizes, but processing is required to decrease the laser beams imprint on smaller scales.
Nouwakpo, S. K., And Others) 2016) [9]	evaluate the capabilities of SfM and TLS on surfaces to exposed acquire large-scale soil surface microscope imaging.	• image acquisition • Overlapping soil surface images were imported into PhotoScan • Define points on GCP images. • DEM generation • Model evaluation using Cloud Compare V2.5 • spatial analysis • Statistical analysis	a discrepancy in height of 5 millimeters between the TLS DEM and the SfM DEM	Point clouds of the extracted model using laser scanning technology were compared with point clouds extracted from SfM technology using Cloud Compare v2.5 software.
Liu, L.Et Al (2022) [10]	The Study Aimed To Evaluate The Soil's Surface Roughness After Ditching Using Terrestrial Laser Scanning.	• Soil Box Design • Prepare The Soil Model • Scan The Model with A Laser Device Before and After Engraving. • Data Processing with Matlab Program • Generate A 3d Digital Model of The Surface. • Surface Statistical Analysis	Rmsh Results Change with Hole Depth	Comparison Between the Depth Calculated in The Field And The Depth Calculated From The Model And Determining The Amount Of Error
Kaźmierowski, C.Et Al (2015) [14]	The objective of present studies is transition from quantifying surface roughness of sample area into quantifying surface roughness for whole field area.	• photo capture • processing was based on Agisoft Photoscan Proffesional 1.1.6 software. • The location of four ground photo mark points were measured. • DEM generation • calculated analysis from DEM using Grassi	The results showed that the average pixel size in the digital image used for photographic processing is about 0.25 cm, meaning about 12 million points that form the calculated point cloud. This corresponds to 19500 points per square meter.	The surface roughness was estimated based on sample regions as bounding squares and based on those samples,
Dirk H. Rieke-Zapp (2005) [19]	The purpose of this study was to develop a method for producing DEMs from soil surfaces that could be updated at high frequency.	• Camera Calibration • Image Acquisition • DEM Generation	DEMs with 3 mm resolution and 1 mm vertical precision were sufficient to achieve erosion measuring goals. With one pixel measuring 0.009 mm, the scale bar (mm) computed length between the observed length and the model length was RMSE = 0.235. RMSE of differences at control points along X = 0.031 mm and Y = 0.042 mm	The BLUH program has been compared to a CDW in A test field with 72 control points provided 28 photographs. Target picture coordinates were measured with a precision higher than 0.02 pixels. According to the findings, the CDW program produced more accurate BLUH results from the identical data set.
Kenarsari, A Et Al (2017) [20]	This Work Aims to Examine The Photogrammetry Approach For Building Three-Dimensional	• Investigations • Static Tire Loading Experiments Using A Single Tire Footprint	This Test Result Demonstrates That Photogrammetry Is A Rather Strong Approach For Simulating Complicated Soil Deformations And Soil	Two Sand Cone Tests Were Conducted to Determine the Volume of The Tire's Footprint for Comparison With The

	Models Of A Tire Footprint To Measure Its Depth, Area, And Volume.	• Single Tire Footprint Volume Measurement and Continuous Tire Footprint Test • Building The Model in Agisoft Photoscan and Placing Markers and Cameras In The Appropriate Places. • Agisoft Photoscan's 3d Representation of The Soil's Surface. • Evaluation Of Photogrammetry Accuracy	Movement Beyond The Frame Region.	Photogrammetry Assessment.
Grundy, L., Ghimire, C., & Snow, V. (2020) [21]	Characterization Of Soil Micro-Topography Using A Depth Camera	• calibration, camera • data acquisition • creating the final 3d point cloud • estimate accuracy and precision, the camera	the relative accuracy was 0.3% at the height camera on the surface of 750mm, while 0.5% at the height camera on the surface of 1500mm. the camera discovered that the height of the undamaged soil was 0.40 mm on average, with a 0.28 mm standard deviation, while the height of the damaged soil was 0.28 mm. the soil that had not been affected measured 13.8 and 0.02 mm in random roughness, while the soil that had been damaged measured 26.0 and 0.04 mm.	linear regression between the theoretical model's area and the one estimated by the 3d camera at 750 mm from the surface, the accuracy of the surfaces is determined.
Suchan, J., & Azam, S. (2021) [22]	System For Controlled Photogrammetric Assessment of Soil Volume and Surface Characteristics.	• Detailed Design • A Sample of The Soil. • Use The Crp Method Of The Soil Model To Take Pictures. • Get Pictures for Modeling. • Using Agisoft Metashape Professional to Process • Google Sketchup Is Used to Make a Sample Cup (Gsu) • Cloudcompare V.2 Is Used to Compare the Two Models (Cc2) • Use Autodesk Civil 3d (Ac3) To Find the Line Where the Two Models Meet.)	The Root Means Square Error (Rmse) Of the Target Score Is A Measure Of How Accurate The Model Is. It Does This by Changing the Model's Coordinate System Along The X, Y, And Z Axes. Rmse Is Between 0.32 And 0.58 Mm. The Error For 1 Pixel Was 0.290–0.629 Pixels.	Using Comparison Cloud, The Researcher Compared the Two Models.
Azizi, A. Et Al (2021) [23]	The goal of this study is to come up with a computerized method based on stereoscopic vision technology that can measure how rough agricultural soils are.	• Soil Preparation To gather image data from tilled soil • Camera calibration using toolbox of MATLAB R2018a software. • Collecting stereo images	1-Camera calibration results 2-The results of evaluating the model by monitoring 5 points and finding the difference between the observed and estimated from the model. RMSE X (Pixel)= 1.07 , RMSE Y (Pixel)= 1.65 , RMSE XY= 2.14	Use the regression equation to evaluate the measured and estimated soil surface roughness
Herodowicz-Mleczak, K. Et Al (2022) [24]	The study's major goal is to develop soil roughness prediction models based on knowledge about tillage practices and soil characteristics.	• Analysis of soil and agricultural maps satellite image and field verification • Registration of soil surface roughness using camera • soil sample describe soil properties. • Creation of DEMs and then calculation of soil surface • Statistical analysis	HSD and T3D (R2 = 0.59), although showing a significant connection, gave distinct information concerning soil surface roughness.	The accuracy was tested by comparing the results of the soil surface roughness assay in the lab with the results of the DEM analysis using TNT Mips software to calculate soil surface roughness indices.
Vinci, A Et Al (2017) [27]	A smartphone camera that uses structure-from-motion reconstruction to	• Study site • Experimental set-up • Parameter camera calibration obtained by Agisoft Lens • SfM image acquisition	Georeferencing errors for SfM were about 0.005 m and for TLS, they were about 0.003 m. (mean values	The SfM model was checked with terrestrial laser scanning (TLS).

	measure how the surface of the soil changes and how much soil is lost due to erosion.	• Photogrammetric processing and generation of point cloud • TLS processing and generation of DEM • Validation of SfM point clouds and DEMs. • Assessing errors of SfM and TLS and SfM validation based on TLS dataset	determined from the two surveys).

6. Result and Discussion

Through Table 1, it is possible to note the accuracy and methodology of each technology with the devices used for each technology, as well as the quality of the cameras and their benefits for each technology, to obtain an accurate three-dimensional model of the soil surface using TLS, CRP, UAV, or video measurement to study the surface properties. The use of TLS laser scanning technology has high accuracy in collecting data in the form of a cloud of dense points. However, TLS still takes a time to scan the area, time to move the laser device, time to install the device in a new location, and time to reset it. Thus, moving the 3D laser may be more complex and costly as compared with other devices used for 3D modelling. The findings of the model were exact and competitive based on the drone-based surveying technique's implementation in real-world create models of surfaces that are difficult to reach due to the beams, .The drone is considered one of the traditional methods because drones can fly in multiple modes and one of the benefits of the image is that it provides a three-dimensional representation of the surface was import them , model, using software GIS or ArcMap analysis quantitative and statistical examination of the models. There are several the limitations in digital Photogrammetry Modeling using Close-Range Photogrammetric (CRP method). One of these limitations is that this approach is difficult and stressful when using it to capture large study areas since it takes so long to cover the region with photographs. However, there are many significances of using CRP for 3D soil modeling. For instance, it is a low-cost system, and needs short processing time as compared with TLS. On the other hand, the videogrammetric approach is highly recommended for 3D soil surface modelling because it is economic and can be used for modelling a large studying area in a shorter time as compared with other 3D modelling methods. Furthermore, by recording the video of the area, it will save the scanner the time spent in the imaging process using the photocopy technique; thus, it can obtain many images when cutting the video into frames, and avoiding returning to the site for re-imaging and filling the gaps that occur in the model. In addition, the accuracy of the videogrammetric approach is efficient and Table 2 shows the characteristics of the methods for generating 3D models, and we note the differences between the techniques used in terms of data collection, type, and cost.

Table 2. 3D model generation methods' characteristics

Properties	CRP	TLS	UAV	Videogrammetry	Reference
Monitoring Of Object	Static	Static	Static	Dynamic using camera one	[14], [27], [30]
3D Coordinate Acquisition	To be derived	Direct as 3D point cloud	To be derived	To be derived	[25], [29]
Data Collection Time	Less Time	Long Time	Less Time	Much less than CRP, TLS, UAV	[28], [30]
Data Quality	Image Resolution	3D data density	Image Resolution	Video Resolution	[25], [30]
Cost Of the Instruments	Low cost	Expensive	Low cost	Low cost	[9], [10], [27]

7. Conclusions

The development of three-dimensional models is currently a hot topic. This essay provides examples of 3D modelling methods and uses. An overview of the theories and methods underlying the creation of 3D models using image- and video-based methodologies is provided. Photogrammetry techniques, whether with digital non-metric cameras or drones, are very accurate in producing three-dimensional models of the soil surface. Still, there are limitations to these techniques, so the skill in image capturing and knowledge of the basic principles in photogrammetry must be available. For example, the overlap and the sequence of arranged pairs of images taken on different days are two basic principles that must be understood. The laser scanning technology used to create 3D models is incredibly precise. Finishing the scanning procedure before processing and creating the 3D model is expensive and complicated. One method that can be utilized to produce a 3D model is videogrammetry. The drawbacks of earlier methods can be fixed with the help of the videogrammetry approach. Because the user's camera may be used, this technique can cut the time needed for data collection and processing while decreasing hardware expenses.

Additionally, advanced hardware and software knowledge is not required for data processing while using videogrammetry. The user can also move around while taking a video of the structure or object using the videogrammetry method. Compared to other technologies, videogrammetry has various benefits, including non-contact, high precision, affordability, and accessibility.

Acknowledgement

Special thanks to the College of Engineering Technology for their help in conducting our research.

Reference

[1] Batakanwa, N., & Lipecki, T. (2020). The use of video camera to create metric 3D model of engineering objects. Geoinformatica Polonica, 19. doi.org/10.24867/07kg05radovic.

[2] Mikhail, E. M., Bethel, J. S., & McGlone, J. C. (2001). Introduction to modern photogrammetry. John Wiley & Sons. doi: 10.12691/jgg-2-3-5

[3] Chong, A. K., Al-Baghdadi, J. A. A., & Alshadli, D. (2014, January). High-definition video cameras for measuring movement of vibrating bridge structure. In International Conference on Vibration and Vibro-acoustics (ICVV2014) (pp. 1-10). University of Southern Queensland.

[4] Alsadik, B. S. A. (2014). Guided close range photogrammetry for 3D modelling of cultural heritage sites. Netherlands: ITC Printing Department. DOI:10.3990/1.9789036537933

[5] Elliot W. J., Laflen J. M., Thomas A. W., Kohl K. D. (1997). "Photogrammetric and rillmeter techniques for hydraulic measurement in soil erosion studies," Transactions of the ASAE, 40(1), pp 157–165 doi: 10.13031/2013.21261) @1997

[6] Nouwakpo, S., Huang, C. H., Frankenberger, J., Bethel, J., & Lafayette, W. (2010, June). A simplified close range photogrammetry method for soil erosion assessment. In 2nd Joint Federal Interagency Conference, Las Vegas, NV (Vol. 27) doi:10.1236/sssaj2011.0148

[7] Hu Y, Fister W, He Y, Kuhn NJ. 2020. Assessment of crusting effects on interrill erosion by laser scanning. PeerJ 8:e8487 https://doi.org/10.7717/peerj.8487

[8] Milenković, M., Pfeifer, N., & Glira, P. (2015). Applying terrestrial laser scanning for soil surface roughness assessment. Remote Sens. 2015, 7(2), 2007-2045; https://doi.org/10.3390/rs70202007

[9] Nouwakpo, S. K., Weltz, M. A., & McGwire, K. (2016). Assessing the performance of structure-from-motion photogrammetry and terrestrial LiDAR for reconstructing soil surface microtopography of naturally vegetated plots. Earth Surface Processes and Landforms, 41(3), 308-322. https://doi.org/10.1002/esp.3787

[10] Liu, L., Bi, Q., Zhang, Q., Tang, J., Bi, D., & Chen, L. (2022, March). Evaluation Method of Soil Surface Roughness after Ditching Operation Based on Wavelet Transform. In Actuators (Vol. 11, No. 3, p. 87). MDPI. https://doi.org/10.3390/act11030087

[11] Lee, S., Choi, Y., 2015. Topographic survey at small-scale open-pit mines using a popular rotary-wing unmanned aerial vehicle (drone). J. Korean Soc. Rock Mech. 25, 462e469.https://doi.org/10.7474/TUS.2015.25.5.462

[12] Winkelmaier, G., Battulwar, R., Khoshdeli, M., Valencia, J., Sattarvand, J., Bahram, P., 2020. Topographically guided UAV for identifying tension cracks using imagebased analytics in open-pit mines. IEEE J. Trans. Ind. Eng. https://doi.org/ 10.1109/TIE.2020.2992011.DOI: 10.1109/TIE.2020.2992011

[13] Zekkos, D., Professor, A., Greenwood, W., Lynch, J., Athanasopoulos-Zekkos, A., Clark, M., 2018. Lessons learned from the application of UAV-enabled structurefrom-motion photogrammetry in geotechnical engineering. Int. J. Geoengin. Case Hist. 4 (4), 254e274.DOI: http://dx.doi.org/10.4417/IJGCH-04-04-03

[14] Kaźmierowski, C., Ceglarek, J., Królewicz, S., Cierniewski, J., Universityc, A. M., Jasiewicz, J., & Wyczałek, M. (2015). Soil surface roughness quantification using DEM obtained from UAV photogrammetry. Geomorphometry for Geosciences, Adam Mickiewicz University in Poznań–Institute of Geoecology and Geoinformation doi:10.13140/RG.2.1.4811.8889

[15] Cleveland, L.J., Wartman, J., 2006. Principles and applications of digital photogrammetry for geotechnical engineering. Site Geomater. Characteriz. ASCE, 128–135.https://doi.org/10.1061/40861(193)16

[16] Kenarsari, A. E., Vitton, S. J., & Beard, J. E. (2017). Creating 3D models of tractor tire footprints using close-range digital photogrammetry. Journal of Terramechanics, 74, 1-11.https://doi.org/10.1016/j.jterra.2017.06.001

[17] Stojic, M., Chandler, J., Ashmore, P. and Luce, J., 1998. The assessment of sediment transport rates by automated digital photogrammetry. Photogrammetric Engineering & Remote Sensing, 64(5): 387–395 DOI:10.1002/(SICI)1096-9837(199901)24:13.0.CO;2-H.

[18] Lascelles, B., Favis-Mortlock, D., Parsons, T. and Boardman, J., 2002. Automated digital photogrammetry: a valuable tool for small-scale geomorphological research for the non-photogrammetrist? Transactions in GIS, 6(1): 5–15. https://doi.org/10.1111/1467-9671.00091

[19] Rieke-Zapp, D. H., & Nearing, M. A. (2005). Digital close-range photogrammetry for measurement of soil erosion. The Photogrammetric Record, 20(109), 69-87. https://doi.org/10.1111/j.1477-9730.2005.00305.x

[20] Abban, B. K., Papanicolaou, A. N., Giannopoulos, C. P., Dermisis, D. C., Wacha, K. M., Wilson, C. G., & Elhakeem, M. (2017). Quantifying the changes of soil surface microroughness due to rainfall impact on a smooth surface. Nonlinear Processes in Geophysics, 24(3), 569-579. https://doi.org/10.5194/npg-24-569-2017.

[21] Grundy, L., Ghimire, C., & Snow, V. (2020). Characterisation of soil micro-topography using a depth camera. MethodsX, 7, 101144.https://doi.org/10.1016/j.mex.2020.101144

[22] Suchan, J., & Azam, S. (2021). Controlled photogrammetry system for determination of volume and surface features in soils. MethodsX, 8, 101368.https://doi.org/10.1016/j.mex.2021.101368

[23] Azizi, A., Abbaspour-Gilandeh, Y., Mesri-Gundoshmian, T., Farooque, A. A., & Afzaal, H. (2021). Estimation of soil surface roughness using stereo vision approach. Sensors, 21(13), 4386.https://doi.org/10.3390/s21134386

[24] Herodowicz-Mleczak, K., Piekarczyk, J., Kaźmierowski, C., Nowosad, J., & Mleczak, M. (2022). Estimating soil surface roughness with models based on the information about tillage practises and soil parameters. Journal of Advances in Modeling Earth Systems, 14(3), e2021MS002578 https://doi.org/10.1029/2021MS002578

[25] Zhu, Z., & Brilakis, I. (2009). Comparison of optical sensor-based spatial data collection techniques for civil infrastructure modeling. Journal of Computing in Civil Engineering, 23(3), 170-177https://doi.org/10.1061/(ASCE)0887-3801(2009)23:3(170).

[26] Remondino, F., & El-Hakim, S. (2006). Image-based 3D modelling: a review. The photogrammetric record, 21(115), 269-291 https://doi.org/10.1111/j.1477-9730.2006.00383.x

[27] Vinci, A., Todisco, F., Brigante, R., Mannocchi, F., & Radicioni, F. (2017). A smartphone camera for the structure from motion reconstruction for measuring soil surface variations and soil loss due to erosion. Hydrology Research, 48(3), 673-685 https://doi.org/10.2166/nh.2017.075.

[28] Laburda, T., Krása, J., Zumr, D., Devátý, J., Vrána, M., Zambon, N., ... & Dostál, T. (2021). SfM-MVS Photogrammetry for Splash Erosion Monitoring under Natural Rainfall. Earth Surface Processes and Landforms, 46(5), 1067-1082 https://doi.org/10.1002/esp.5087

[29] Ortiz-Coder, P., & Sánchez-Ríos, A. (2020). An integrated solution for 3D heritage modeling based on videogrammetry and V-SLAM technology. Remote Sensing, 12(9), 1529 https://doi.org/10.3390/rs12091529.

[30] Deliry, S. I., & Avdan, U. (2021). Accuracy of unmanned aerial systems photogrammetry and structure from motion in surveying and mapping: A review. Journal of the Indian Society of Remote Sensing, 49(8), 1997-2017 https://doi.org/10.1007/s12524-021-01366.